Research Report IDE-0131, September 2001

Symmetry derivatives of Gaussians illustrated by cross tracking

Josef Bigun and Tomas Bigun

IDE

Sektionen för Informationsvetenskap,
Data- och Elektroteknik

School of Information Science, Computer
and Electrical Engineering

Högskolan i Halmstad/Halmstad University
Box 823, S-301 18 Halmstad, Sweden
e-mail: ide@hh.se http://www.hh.se

Symmetry derivatives of Gaussians illustrated by cross tracking

Josef Bigun*
Halmstad University
P.O. Box 823
SE-301 18 Halmstad
www.hh.se

Tomas Bigun
TietoEnator ArosTech AB
Storg. 3
SE-582 23 Linköping
www.tietoenator.com

Abstract

We propose a family of complex differential operators, symmetry derivatives, for pattern recognition in images. We present three theorems on their properties as applied to Gaussians. These show that all orders of symmetry derivatives of Gaussians yield compact expressions obtained by replacing the original differential polynomial with an ordinary polynomial. Just like Gaussians, the symmetry derivatives of Gaussians are (form) invariant to Fourier transform, that is they are rescaled versions of the original. As a result, the symmetry derivatives of Gaussians are closed under the convolution operator, i.e. they map on a member of the family when convolved with each other. Since Gaussians are utilized extensively in image processing, the revealed properties have practical consequences, e.g. when designing filters and filtering schemes that are unbiased w.r.t. orientation (isotropic). A use of these results is illustrated by an application: tracking the cross markers in long image sequences from vehicle crash tests. The implementation and the results of this application are discussed in terms of the theorems presented, along with conclusions.

1 Introduction

Let the *first symmetry derivative* be defined as

$$D_x + iD_y = \frac{\partial}{\partial x} + i\frac{\partial}{\partial y} \tag{1}$$

which resembles the ordinary gradient in 2-D. However, when it is applied to a scalar function $f(x, y)$, it results in a complex field instead of a vector field. Most importantly, it is

*Corresponding author

possible to produce new operators by taking integer powers of it i.e.:

$$\begin{aligned}(D_x + iD_y)^2 &= (D_x^2 - D_y^2) + i(2D_xD_y)\\ (D_x + iD_y)^3 &= (D_x^3 - 3D_xD_y^2) + i(3D_x^2D_y - D_y^3)\\ &\dots\end{aligned}$$

We will call the operator, $(D_x + iD_y)^n$ *the n'th symmetry derivative* .

In an analogous manner we define *the first conjugate symmetry derivative* as

$$D_x - iD_y = \frac{\partial}{\partial x} - i\frac{\partial}{\partial y} \tag{2}$$

and *the n'th conjugate symmetry derivative* as $(D_x - iD_y)^n$.

Some novel properties of the n'th symmetry derivatives as applied to Gaussian functions is the subject of this paper. The analogies of the presented results also exist for the n'th conjugate symmetry derivatives. But these will neither be mentioned nor proven any further than those for the n'th symmetry derivatives because of the straight forward parallelism that exists between the two.

The rationale behind calling the differential operator $(D_x + iD_y)^n$ as n'th symmetry derivative stems from its use in symmetry modeling and detection in gray-scale image analysis. Patterns with iso-gray curves being straight parallel lines in a coordinate system that is harmonic, have previously been studied for recognition purposes and a total least square algorithm (linear symmetry algorithm) for their detection has been suggested, [5, 1, 3]. A pair of harmonic coordinates has the property of consisting of transformation functions that are locally orthogonal to each other. The scheme for recognizing any iso-gray curve of a harmonic pattern consists of "smoothing" the square of the first symmetry derivative of the image with a complex filter that resembles the various symmetry derivatives of Gaussians that will be discussed here. The produced vector fields have a remarkably different sense, [14], than the (edge) orientation fields produced by linear symmetry method in Cartesian coordinates. Depending on the coordinate system chosen, i.e. the filtering that has been applied, the directions of such fields have interpretations that include the symmetry axis orientation of a parabola, the degree of chirality (sense of spirals, circularity versus radiality), presupposed by [14, 23, 15], and the rotation angle of a cross.

In the Cartesian coordinate system, the linear symmetry theory is the mathematical basis of creating dense complex vector (tensor) fields representing local orientation and certainties of straight lines. Some applications are illustrated by texture [30, 6] and finger print analysis as well as image enhancement, [18]. However, when the method is applied to other (harmonic) coordinate systems efficient implementation becomes a non-trivial issue. For illustration, in Section 3, we will elaborate on one such coordinate system that is not Cartesian but yet harmonic.

Early efforts on invariance in pattern recognition are the works of [19, 13, 7] although their formulations use moments in the spatial domain and that these could only be applied to represent global shape of binary objects. By contrast, the shape representations in this paper utilize differential invariants applied to gray scale images. An extension of the linear symmetry theory to 3-D and higher dimensions has also been done (by [5] and later by [24] in the the Gabor space, as well as by [16] in curvilinear coordinates of arbitrary dimensions), but

this has been possible only by using the non-commutative matrix/tensor fields, and not the commutative complex number field discussed here. However, thanks to the commutativity of the complex numbers i) orientation of multi-orientation textures, e.g. fish and snake skin, can be estimated within an extension of linear symmetry theory, [4], ii) the the resulting complex fields generate the optimal orientation, in the total least square error sense, explicitly even in the simultaneous presence of multi orientations.

In image analysis the Gaussian function of the 2-D normal distribution

$$g^{\{\sigma^2\}}(x,y) = \frac{1}{2\pi\sigma^2}\exp(-\frac{x^2+y^2}{2\sigma^2}) \tag{3}$$

and its derivatives have generally been used when constructing isotropic linear filters. A continuous linear operator $\mathbf{T}$ can be translated to the discrete domain by representing the continuous signal to be acted upon as a discrete sum of shifted interpolation functions weighted by the function samples and then acting on the discrete sum,

$$\mathbf{T}f(x,y) = \sum_j f_j 2\pi\sigma^2 \mathbf{T}g^{\{\sigma^2\}}(x-x_j, y-y_j) \tag{4}$$

Here the factor $2\pi\sigma^2$ has been utilized to normalize the maxima of the interpolation functions so that these attain the value 1. Sampling the result, which is continuous, results in a discrete convolution between the discrete image and a discrete filter obtained by sampling $\mathbf{T}g$, which becomes the discrete representation of $\mathbf{T}$. In image analysis, the use of Gaussians is due to their valuable properties, in particular to their:

1. directional isotropy, i.e. in polar coordinates they depend on radius only,
2. separability in x and y coordinates, and
3. simultaneous concentration in the spatial and the frequency domain.

These, together with the inexpensiveness of floating point arithmetics, increasingly make the Gaussians the prime choice in Finite Impulse Response (FIR) filter implementation of the linear operators, including edge [29, 10, 9], orientation vector fields [5, 22], and singularity points detection schemes [5, 17, 1, 2, 11, 3]. Here we note that the "lack" of linear symmetry, which is measured as a quotient relationship between the eigen values suggested in [5], is identical to the quotient suggested by the corner detection scheme suggested by [17]. The linear symmetries will be discussed in some detail in Sections 2 and 3.

The work of [28] provides a valuable investigation on statistics of angular data which is related to issues discussed in this paper. Another relevant contribution, though connected to image tensor fields and linear symmetries at first hand, is the motion estimation technique suggested by [27]. They use the inverse of the auto-correlation matrix of the first order spatial partial derivatives of an image in a context of solving an over determined equation system.

Of course other alternatives to the Gaussian interpolator exist when discretizing continuous operators, e.g. B-splines [31, 20]. These, in particular splines, are widely used in applications. However when orientation isotropy and separability are of significant value, the non-Gaussian interpolators can only approximate the properties of the Gaussians. Consequently, the Gaussians play an important role even when designing non-Gaussian interpolators, since these interpolators are often desired to be similar to Gaussians. Besides interpolation, the Gaussians are used in scale [8, 32, 25, 26, 12] analysis. This wide adoption as

in image analysis tool is, in addition to property 3 which produces compact filters having no ringing effects close to sharp discontinuities, due to that the exponential function is the only continuous function having property 1 and 2:

$$\exp(x^2 + y^2) = \exp(x^2)\exp(y^2) \tag{5}$$

This yields separable and thereby fast implementations of FIR filters that can outperform the use of FFT in computational efficiency.

In the next chapter we will present some properties of the n'th symmetry derivative when applied to Gaussians. In Section 3 we illustrate these properties in the context of a concrete application, tracking markers in crash tests, and discuss the results. In Section 4 the main conclusions will be presented.

2 Symmetry derivatives of Gaussians

We apply the p'th symmetry derivative to the Gaussian and call the result $\mu^{\{p,\sigma^2\}}$:

$$\mu^{\{p,\sigma^2\}}(x,y) = (D_x + iD_y)^p g^{\{\sigma^2\}}(x,y) \tag{6}$$

It is clear that $\mu^{\{p,\sigma^2\}}$ can be obtained by certain linear combinations of the ordinary partial derivatives of a Gaussian. However, these specific linear combinations yield a remarkable simplicity that we will express by a theorem.

First, let us define the polynomial Q as

$$Q(q) = \sum_{n=0}^{N-1} a_n q^n \tag{7}$$

where q is a general variable e.g. $q = D_x + iD_y$ yields a differential operator:

$$Q(D_x + iD_y) = \sum_{n=0}^{N-1} a_n (D_x + iD_y)^n \tag{8}$$

whereas $q = x + iy$ gives a polynomial:

$$Q(x + iy) = \sum_{n=0}^{N-1} a_n (x + iy)^n. \tag{9}$$

Theorem 1 *The differential operator $D_x + iD_y$, the scalar $-\frac{x+iy}{\sigma^2}$ as well as the polynomials of them, act on a Gaussian in an identical manner:*

$$Q(D_x + iD_y) g^{\{\sigma^2\}}(x,y) = Q(\frac{-x}{\sigma^2} + i\frac{-y}{\sigma^2}) g^{\{\sigma^2\}}(x,y) \tag{10}$$

In the special case of the p'th symmetry derivative, i.e. $Q(q) = q^p$, applied to a Gaussian the result yields

$$\mu^{\{p,\sigma^2\}}(x,y) = (D_x + iD_y)^p g^{\{\sigma^2\}}(x,y) = (\frac{-x}{\sigma^2} + i\frac{-y}{\sigma^2})^p g^{\{\sigma^2\}}(x,y) \tag{11}$$

Proof

We prove the theorem by induction for the special case first.

1. Equation (11) holds for $p = 1$.
2. Assume (induction) that equation (11) is true for $p = p_0$, for some $p_0 > 1$.
3. Then

$$\begin{aligned}\mu^{\{p_0+1,\sigma^2\}}(x,y) &= \frac{1}{2\pi\sigma^2}(D_x + iD_y)(D_x + iD_y)^{p_0}\exp(-\frac{x^2+y^2}{2\sigma^2}) \\ &= \frac{1}{2\pi\sigma^2}(D_x + iD_y)[(\frac{-x}{\sigma^2} + i\frac{-y}{\sigma^2})^{p_0}\exp(-\frac{x^2+y^2}{2\sigma^2})] \quad (12)\end{aligned}$$

where we indicated by brackets [] the terms on which the differential operators act, is obtained by applying the induction assumption (Point 2). Consequently and by using the chain rule as well as the linearity of the partial differential operators we obtain,

$$\begin{aligned}\mu^{\{p_0+1,\sigma^2\}}(x,y) &= \frac{1}{2\pi\sigma^2}[(D_x + iD_y)(\frac{-x}{\sigma^2} + i\frac{-y}{\sigma^2})^{p_0}]\exp(-\frac{x^2+y^2}{2\sigma^2})\cdots \\ &\quad + \frac{1}{2\pi\sigma^2}(\frac{-x}{\sigma^2} + i\frac{-y}{\sigma^2})^{p_0}[(D_x + iD_y)\exp(-\frac{x^2+y^2}{2\sigma^2})] \quad (13)\end{aligned}$$

By repeated applications of the algebraic rules that govern the differential operators, we obtain

$$\begin{aligned}\mu^{\{p_0+1,\sigma^2\}}(x,y) &= \frac{1}{2\pi\sigma^2}[D_x(\frac{-x}{\sigma^2} + i\frac{-y}{\sigma^2})^{p_0} + iD_y(\frac{-x}{\sigma^2} + i\frac{-y}{\sigma^2})^{p_0}]\exp(-\frac{x^2+y^2}{2\sigma^2})\cdots \\ &\quad + \sigma^2(\frac{-x}{\sigma^2} + i\frac{-y}{\sigma^2})^{p_0}(\frac{-x}{\sigma^2} + i\frac{-y}{\sigma^2})\exp(-\frac{x^2+y^2}{2\sigma^2}) \\ &= \frac{1}{2\pi\sigma^2}(p_0(\frac{-1}{\sigma^2})(\frac{-x}{\sigma^2} + i\frac{-y}{\sigma^2})^{p_0-1} + i^2 p_0(\frac{-1}{\sigma^2})(\frac{-x}{\sigma^2} + i\frac{-y}{\sigma^2})^{p_0-1})\cdots \\ &\quad \times\exp(-\frac{x^2+y^2}{2\sigma^2}) + \frac{1}{2\pi\sigma^2}(\frac{-x}{\sigma^2} + i\frac{-y}{\sigma^2})^{p_0+1}\exp(-\frac{x^2+y^2}{2\sigma^2}) \\ &= \frac{1}{2\pi\sigma^2}(\frac{-x}{\sigma^2} + i\frac{-y}{\sigma^2})^{p_0+1}\exp(-\frac{x^2+y^2}{2\sigma^2}) \quad (14)\end{aligned}$$

Consequently when it holds for $p = p_0$, equation (11) will also hold for $p = p_0 + 1$.

Now we turn to the general case

$$\begin{aligned}Q(D_x + iD_y)\frac{1}{2\pi\sigma^2}\exp(-\frac{x^2+y^2}{2\sigma^2}) &= \frac{1}{2\pi\sigma^2}[\sum_{n=0}^{N-1} a_n(D_x + iD_y)^n]\exp(-\frac{x^2+y^2}{2\sigma^2}) \\ &= \frac{1}{2\pi\sigma^2}\sum_{n=0}^{N-1} a_n[(D_x + iD_y)^n\exp(-\frac{x^2+y^2}{2\sigma^2})] \\ &= \frac{1}{2\pi\sigma^2}\sum_{n=0}^{N-1} a_n(\frac{-x}{\sigma^2} + i\frac{-y}{\sigma^2})^n\exp(-\frac{x^2+y^2}{2\sigma^2}) \\ &= Q(\frac{-x}{\sigma^2} + i\frac{-y}{\sigma^2})\frac{1}{2\pi\sigma^2}\exp(-\frac{x^2+y^2}{2\sigma^2})\end{aligned}$$

in which the linearity of the sums of derivative operators and equation (11) has been utilized■

That the Fourier transformation of a Gaussian is also a Gaussian has widely been known and exploited in computer and information related sciences. It turns out that this elegant simplicity is generalizable by use of symmetry derivatives. We state it in the original theorem that follows.

Theorem 2 *The symmetry derivatives of a Gaussian are Fourier transformed on themselves i.e.*

$$\begin{aligned}\mathcal{F}[\mu^{\{p,\sigma^2\}}](\omega_x,\omega_y) &= \int\int \mu^{\{p,\sigma^2\}}(x,y)\exp(-i\omega_x x - i\omega_y y)dxdy \\ &= 2\pi\sigma^2(\frac{-i}{\sigma^2})^p\mu^{\{p,\frac{1}{\sigma^2}\}}(\omega_x,\omega_y) \end{aligned} \tag{15}$$

Proof By taking the Fourier Transform of equation (11) we obtain

$$\begin{aligned}\mathcal{F}[\mu^{\{p,\sigma^2\}}](\omega_x,\omega_y) &= \mathcal{F}[\frac{1}{2\pi\sigma^2}(D_x+iD_y)\cdots(D_x+iD_y)\exp(-\frac{x^2+y^2}{2\sigma^2})](\omega_x,\omega_y) \\ &= (i\omega_x + i\cdot i\omega_y)\cdots(i\omega_x+i\cdot i\omega_y)\mathcal{F}[\frac{1}{2\pi\sigma^2}\exp(-\frac{x^2+y^2}{2\sigma^2}](\omega_x,\omega_y) \\ &= (i)^p(\omega_x+i\omega_y)\cdots(\omega_x+i\omega_y)\exp(-\frac{\omega_x^2+\omega_y^2}{2\frac{1}{\sigma^2}}) \\ &= \frac{1}{\sigma^2}(i)^p(\omega_x+i\omega_y)^p\sigma^2\exp(-\frac{\omega_x^2+\omega_y^2}{2\frac{1}{\sigma^2}}) \\ &= \frac{1}{\sigma^2}(i)^p(\frac{-1}{\sigma^2})^p(-\sigma^2\omega_x - i\sigma^2\omega_y)^p\sigma^2\exp(-\frac{\omega_x^2+\omega_y^2}{2\frac{1}{\sigma^2}}) \\ &= \frac{2\pi}{2\pi\sigma^2}(\frac{-i}{\sigma^2})^p\sigma^2(D_x+iD_y)^p\exp(-\frac{\omega_x^2+\omega_y^2}{2\frac{1}{\sigma^2}}) \\ &= 2\pi\sigma^2(\frac{-i}{\sigma^2})^p\mu^{\{p,\frac{1}{\sigma^2}\}}(\omega_x,\omega_y) \end{aligned} \tag{16}$$

which is what had to be proven■

As an immediate consequence of this theorem, we obtain the following lemma

Lemma 1 *The function $\mu^{\{p,\sigma^2\}}$ with $\sigma^2 = 1$ is an eigen function of the 2-D Fourier transform with the eigen-value $2\pi(-i)^p$ i.e.*

$$\mathcal{F}[\mu^{\{p,1\}}](\omega_x,\omega_y) = 2\pi(-i)^p\mu^{\{p,1\}}(\omega_x,\omega_y) \tag{17}$$

The following theorem states that the convolution of two symmetry kernels results in another symmetry kernel, with the two symmetry orders, and the two variances adding up independently:

Theorem 3 *the symmetry derivatives of Gaussians are closed under the convolution operator. In particular the order and the variance parameters add under convolution.*

$$\mu^{\{p_1,\sigma_1^2\}} * \mu^{\{p_2,\sigma_2^2\}} = \mu^{\{p_1+p_2,\sigma_1^2+\sigma_2^2\}} \tag{18}$$

Proof Convolution in the Fourier transform domain reduces to an ordinary multiplication:

$$\mu^{\{p_1,\sigma_1^2\}} * \mu^{\{p_2,\sigma_2^2\}} \leftrightarrow \mathcal{F}[\mu^{\{p_1,\sigma_1^2\}}]\mathcal{F}[\mu^{\{p_2,\sigma_2^2\}}] \tag{19}$$

Therefore by using (15) we note that

$$\mathcal{F}[\mu^{\{p_1,\sigma_1^2\}}](\omega_x,\omega_y) = 2\pi(\frac{-i}{\sigma_1^2})^{p_1}\sigma_1^2\mu^{\{p_1,\frac{1}{\sigma_1^2}\}}(\omega_x,\omega_y) \tag{20}$$

$$\mathcal{F}[\mu^{\{p_2,\sigma_2^2\}}](\omega_x,\omega_y) = 2\pi(\frac{-i}{\sigma_2^2})^{p_2}\sigma_2^2\mu^{\{p_2,\frac{1}{\sigma_2^2}\}}(\omega_x,\omega_y) \tag{21}$$

and form their product by using (11):

$$\begin{aligned}
&\mathcal{F}[\mu^{\{p_1,\sigma_1^2\}}]\cdot\mathcal{F}[\mu^{\{p_2,\sigma_2^2\}}] = 2\pi(\frac{-i}{\sigma_1^2})^{p_1}\sigma_1^2\mu^{\{p_1,\frac{1}{\sigma_1^2}\}}(\omega_x,\omega_y)\cdot 2\pi(\frac{-i}{\sigma_2^2})^{p_2}\sigma_2^2\mu^{\{p_2,\frac{1}{\sigma_2^2}\}}(\omega_x,\omega_y)\\
= \;& 2\pi\sigma_1^2(\frac{-i}{\sigma_1^2})^{p_1}(-\sigma_1^2)^{p_1}(\omega_x+i\omega_y)^{p_1}\frac{1}{2\pi\sigma_1^2}\exp(-\sigma_1^2\frac{\omega_x^2+\omega_y^2}{2})\cdots\\
& \times 2\pi\sigma_2^2(\frac{-i}{\sigma_2^2})^{p_2}(-\sigma_2^2)^{p_2}(\omega_x+i\omega_y)^{p_2}\frac{1}{2\pi\sigma_2^2}\exp(-\sigma_2^2\frac{\omega_x^2+\omega_y^2}{2})\\
= \;& (\frac{-i}{\sigma_1^2})^{p_1}(\frac{-i}{\sigma_2^2})^{p_2}(-\sigma_1^2)^{p_1}(-\sigma_2^2)^{p_2}(\omega_x+i\omega_y)^{p_1+p_2}\exp(-\frac{\omega_x^2+\omega_y^2}{2\frac{1}{\sigma_1^2+\sigma_2^2}})
\end{aligned} \tag{22}$$

Canceling the redundant terms allows us to write the product as

$$\begin{aligned}
&\mathcal{F}[\mu^{\{p_1,\sigma_1^2\}}]\cdot\mathcal{F}[\mu^{\{p_2,\sigma_2^2\}}] = (i)^{p_1+p_2}(\omega_x+i\omega_y)^{p_1+p_2}\exp(-\frac{\omega_x^2+\omega_y^2}{2\frac{1}{\sigma_1^2+\sigma_2^2}})\\
= \;& \frac{2\pi(\sigma_1^2+\sigma_2^2)}{2\pi(\sigma_1^2+\sigma_2^2)}(i)^{p_1+p_2}(\omega_x+i\omega_y)^{p_1+p_2}\exp(-\frac{\omega_x^2+\omega_y^2}{2\frac{1}{\sigma_1^2+\sigma_2^2}})\frac{(-\sigma_1^2-\sigma_2^2)^{p_1+p_2}}{(-\sigma_1^2-\sigma_2^2)^{p_1+p_2}}\\
= \;& 2\pi(\sigma_1^2+\sigma_2^2)(\frac{i}{-\sigma_1^2-\sigma_2^2})^{p_1+p_2}\mu^{\{p_1+p_2,\frac{1}{\sigma_1^2+\sigma_2^2}\}}(\omega_x,\omega_y)
\end{aligned} \tag{23}$$

Remembering, (19) we now inverse Fourier transform (23) by using (15) and obtain

$$\mu^{\{p_1,\sigma_1^2\}} * \mu^{\{p_2,\sigma_2^2\}} = \mu^{\{p_1+p_2,\sigma_1^2+\sigma_2^2\}} \tag{24}$$

that completes the proof■

Definition 1 *Let the scalar product, $<,>$, of two functions f, g, both defined on the entire plane, be*

$$< f,g >= \int\int f^*(x,y)g(x,y)dxdy$$

. Here it is assumed that the integral exists (at least as a distribution) when taken over the entire plane. Then the complex scalar I_{pq}

$$I_{pq} =< m(x,y),(x+iy)^p(x-iy)^q > \tag{25}$$

with p and q being non-negative integers, is said to be the complex moment p,q of the function m. The order number and the symmetry number of a complex moment are $p+q$ and $p-q$ respectively.

The following theorem is stated without proof for the sake of completeness and since we will need it in the next section. It has previously been applied to the power spectrum of a local image for the purpose of estimating the "orientation" parameter of various symmetric patterns. Here, the orientation parameter has a different sense depending on the coordinate system it is defined in. We refer to [5] for its proof for line patterns in Cartesian coordinates and [3] for its proof for general patterns in harmonic coordinates.

Theorem 4 (Linear Symmetry) *Assume that the second order complex moments, I_{20}, I_{11}, of a planar real mass distribution, $0 \leq m(x,y)$, are finite scalars and that the origin is in the mass center i.e. $I_{10} = I_{01} = 0$. Then the minimum inertia (total least square error) axis of the mass is given by I_{20} and the corresponding inertia is given by $\lambda_{min} = I_{11} - |I_{20}|$:*

$$\begin{aligned} I_{11} &= < m(x,y), |x+iy|^2 >= \lambda_{max} + \lambda_{min} \\ I_{20} &= < m(x,y), (x+iy)^2 >= (\lambda_{max} - \lambda_{min}) \exp(i2\varphi_{\bar{k}_{min}}) \end{aligned}$$

Here λ_{max}, and λ_{min} are the eigenvalues of the inertia matrix of the mass whereas $\varphi_{\bar{k}_{min}}$ is the direction angle of the eigenvector $\bar{k}_{min}$ that corresponds to λ_{min}. The linear symmetry axis is $\bar{k}_{min}$. The direction of the maximum inertia axis is represented similarly by $-I_{20}$:

$$-I_{20} = (\lambda_{max} - \lambda_{min}) \exp(i2\varphi_{\bar{k}_{max}})$$

In image analysis applications $m(x,y)$ is the power spectrum $|F(\omega_x, \omega_y)|^2$ where F is the Fourier transform of a spatial pattern $f(x,y)$ and the variables x, and y are general harmonic coordinates. In the next section we will use such a coordinate system to model cross-markers. The name linear symmetry is motivated by that the theorem enables to find the symmetry axis of the (parallel) straight line patterns which have a power spectrum concentrated to a Dirac line.

3 An application: symmetry tracker

In vehicle crash tests, the test event is filmed with a high speed camera in order to quantify the impact of various parameters on human safety, including mechanical construction, accident types, and human behavior. A significant aid in this process has been the quantification of the test events by tracking the moving objects accurately. To that end special markers have been painted or sticked to objects, e.g. the body parts of a human model. A common marker is the "cross" which allows to quantify the planar position of an object as well as its planar rotation in individual frames, see Figure 1. Recently accurate automatic tracking of objects in digitized image sequences has attracted significant interest from performers of the tests. This section describes how linear symmetry theorem together with the theorems on symmetry derivatives of Gaussians, allowed a real-time implementation of cross tracking via a filtering scheme that has been in use since 1997 but unpublished until now.

3.1 Model: linear symmetry in hyperbolic coordinates

The cross markers has to be tracked across numerous frames (in the order of hundreds to thousands) of high resolution digitized films, so that the tracking had to be robust in the

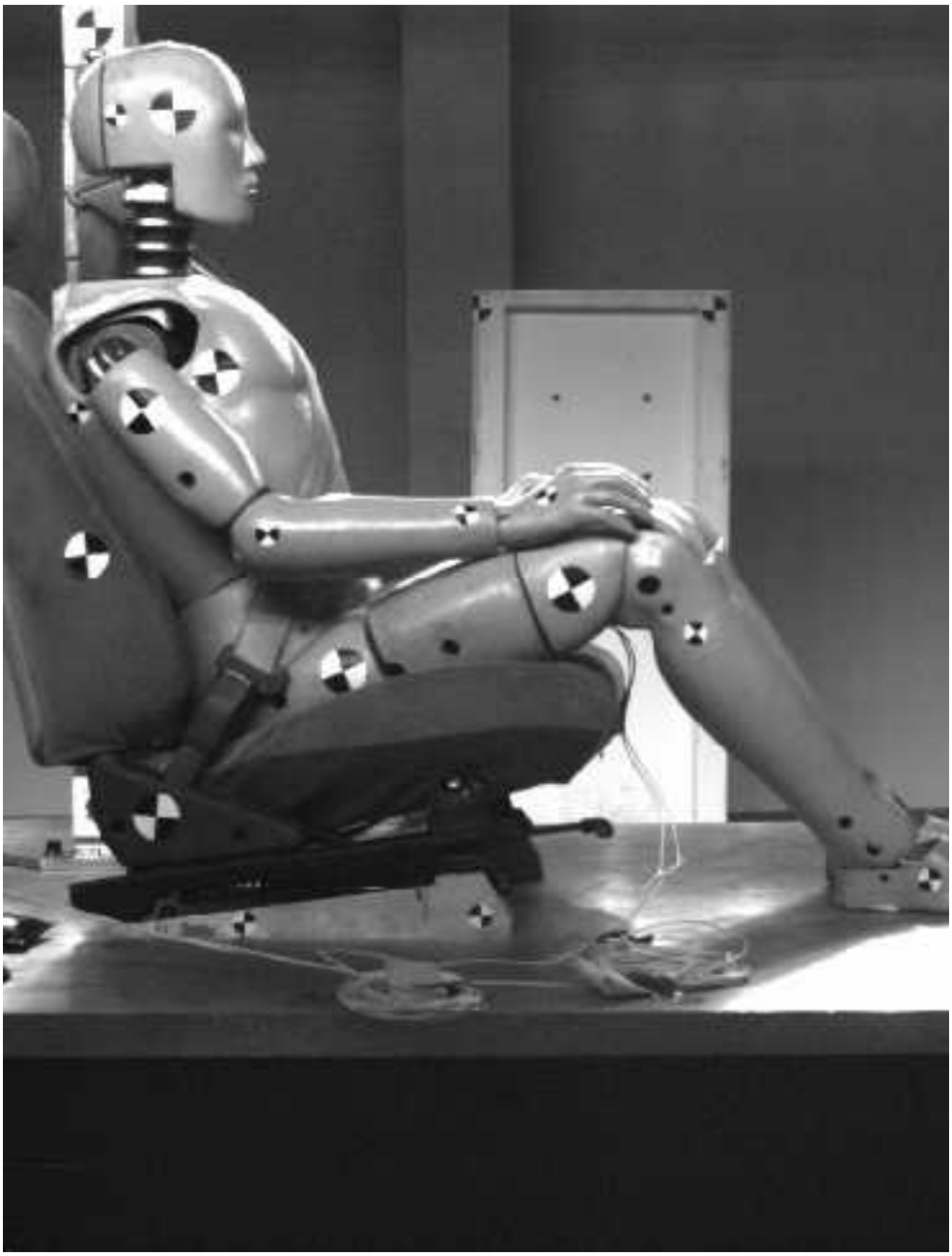

Figure 1: The first frame of an image sequence in which cross markers should be tracked.

sense that detection should be rapid (preferably near real-time) and precise in every frame despite significant rotation and change of contrast. To that end, the cross pattern has been modeled via the hyperbolic patterns:

$$\sin(2\theta)(x^2 - y^2) - \cos(2\theta)2xy = Constant \tag{26}$$

where θ is the angle representing the direction of an asymptote. By changing θ the orientation of the cross pattern can be controlled, see Figure 2 and 3. However, the angle θ is not unique. Due to the 4 folded symmetry, any of the angles, θ, $\theta + \frac{\pi}{4}$, $\theta + \frac{2\pi}{4}$ and $\theta + \frac{3\pi}{4}$ are equally good representations of the cross orientation. Instead the cross orientation can be uniquely represented by 4θ where θ is the angle representing any of the four directions defined by the two asymptotes. In other words, 4θ, or $\cos(4\theta)$, and $\sin(4\theta)$ are the unknown parameters of the orientation determination problem. This problem is equivalent to fit a line to the iso-curves of a candidate image, expressed in the hyperbolic coordinate system, Figure 3:

$$\xi = x^2 - y^2 \tag{27}$$

$$\eta = 2xy \tag{28}$$

Any 2-D pattern generated by the one dimensional function $f(t)$ via the substitution $t = a\xi + b\eta$

$$f(a(x^2 - y^2) + b(2xy)) \tag{29}$$

will have two hyperbolic asymptotes (centered at the origin of the current neighborhood) possessing a precise orientation determined by $\tan^{-1}(-b, a)$. The ξ, η coordinates system above is harmonic since the curves generated by $\xi = constant_1$ are orthogonal to those generated by $\eta = constant_2$. The iso-gray curves of patterns generated by Equation (29) consist of (parallel) straight lines in the hyperbolic coordinates. The one dimensional function f is allowed to have discontinuities e.g. the step function

$$f(t) = \chi(t) = \begin{cases} 1, & \text{if } t > 0; \\ 0, & \text{otherwise.} \end{cases} \tag{30}$$

is permitted, since the linear symmetry theorem does not put restrictions on the "mass" m, in our case the energy of the Fourier spectrum $|F|^2$, other than the integrals must exist finitely, i.e. the energy must be finite.

The choice of the function f as the step function χ, incidentally generates an exact model of the cross-patterns used in the crash tests, Figure 2. Consequently the corresponding algorithm finding linear symmetry orientation will be exact even for ideal cross markers as far as their positions and orientations are concerned despite that the crosses are the asymptotes of the hyperbolic coordinate transformations used in the model.

The problem of linear symmetry orientation estimation is the same as that of fitting a line to the power spectrum of the pattern expressed in (ξ, η) coordinate system. This is because, regardless of f, the power spectrum of $f(a\xi + b\eta)$ is concentrated to a line, namely $\delta(b\omega_\xi - a\omega_\eta)$ where ω_ξ and ω_η are the frequency variables of the Fourier transformation which is taken w.r.t. the variables ξ and η. To be precise, in the ideal case of existence of perfect linear symmetry the particular one dimensional f that generates the hyperbolic pattern has no influence on the direction of the energy concentration. In the non-ideal case, F will of course not be perfectly concentrated to a line but will have a certain spread, influencing

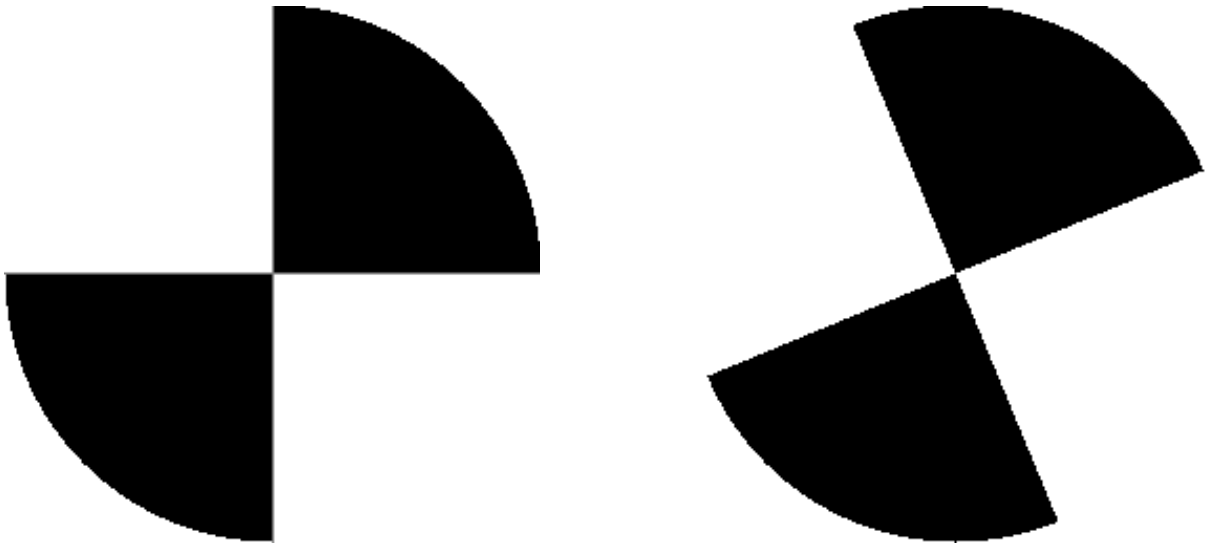

Figure 2: The ideal model of a cross marker obtained by $\chi(\sin(2\theta)\xi - \cos(2\theta)\eta)$. On the left $\theta = 0$ on the right $\theta = \frac{\pi}{8}$ is displayed.

the certainty and the accuracy of the orientation estimation. For example any hyperbolic pattern with an asymptotic direction $\theta = \frac{\pi}{8}$ has an energy that is concentrated to the same oblique line illustrated in Figure 3 bottom-right. As a consequence of this the energy of the ideal cross-marker in Figure 2-Right, will be confined to the same oblique line of Figure 3-Bottom-Right. For the purpose of fitting a line to the power spectrum of a candidate pattern, we will make use of Theorem 4. It will enable us to do the fitting without coordinate transformations or Fourier transformations in these coordinates.

3.2 Implementation and experiments

By using the Parseval theorem, i.e. the scalar products are conserved under the Fourier transform, and the linear symmetry theorem we can solve the line fitting problem in the spatial domain (first in the ξ, η coordinate system, and then in the x, y coordinate system by substitution) via by the equations,

$$I_{20} = \int\int ((D_\xi + iD_\eta)f)^2 d\xi d\eta = \int\int \frac{(x-iy)^2}{|x-iy|^2}((D_x + iD_y)f)^2 dxdy \quad (31)$$

$$I_{11} = \int\int |((D_\xi + iD_\eta)f^2| d\xi d\eta = \int\int |(D_x + iD_y)f|^2 dxdy \quad (32)$$

where f is the (local) spatial image, which only in the ideal case is a one dimensional function of the type given by Equation (29). However, if f happens to conform to Equation (29) then the fit will be without error. In these equations the argument of I_{20} yields the orientation of the cross, 4θ, whereas the magnitude of I_{20} is the difference between the largest and the least square error. The I_{11} is a real scalar that is non-negative and it represents the sum of

the largest and the least square error in the fit. As a consequence of this, the ideal case of a fit without error will be indicated by $|I_{20}| = I_{11}$.

The error which is invariant to rotation of the cross marker, will be used to estimate the position parameter. In order that a machine vision system can determine that the lowest achieved error in the current image is small, one should have an idea of what a large error is, given an image. Here this could be achieved by comparing the least error with the largest error, via $|I_{20}|$ since in an unsatisfactory fit there would not be a large difference between the best and the worst fit. Therefore $\lambda_{max} - \lambda_{min}$ could potentially be used as the likelihood or the certainty for the current image to be a cross-pattern. However, this likelihood measure is not good enough for the needs of our tracker which has to be insensitive against contrast variances of the cross marker. This is because, $|I_{20}|$ still depends on the total energy of the power spectrum, e.g. if m in (25) increases with a multiplicative constant, $C \cdot m$, so does $|I_{20}|$. Here we have used

$$C_r = \frac{\lambda_{max} - \lambda_{min}}{\lambda_{max} + \lambda_{min}} = \frac{|I_{20}|}{I_{11}} \leq 1 \tag{33}$$

which attains its maximum value if and only if $\lambda_{min} = 0$, as the likelihood (certainty) of a cross-marker position. It is of course possible to construct other similar measures by using λ_{min}, and λ_{max} provided that such an expression is invariant to rotation and contrast changes. Neighborhoods that contain cross markers have higher certainties, as compared to those which do not. This in turn allows to track cross markers.

In order to compute I_{20} and I_{11} the square of the first symmetry derivative is needed. The first symmetry derivative can be obtained via convolutions if Gaussians are assumed to be the interpolation functions when representing the continuous image $f(x, y)$ via its samples $f_k = f(x_k, y_k)$:

$$\begin{aligned}
(D_x + iD_y)f(x,y) &= (D_x + iD_y)\sum_k f(x_k, y_k) 2\pi\sigma_1^2 g^{\{\sigma_1\}}(x - x_k, y - y_k) && (34)\\
&= 2\pi\sigma_1^2 \sum_k f(x_k, y_k)(D_x + iD_y) g^{\{\sigma_1\}}(x - x_k, y - y_k) && (35)\\
&= 2\pi\sigma_1^2 \sum_k f(x_k, y_k)\mu^{\{1,\sigma_1\}}(x - x_k, y - y_k) && (36)
\end{aligned}$$

Consequently the first order symmetry derivative discretized on the original grid is given by

$$\begin{aligned}
(D_x + iD_y)f(x_l, y_l) &= 2\pi\sigma_1^2 \sum_k f(x_k, y_k)\mu^{\{1,\sigma_1\}}(x_{l-k}, y_{l-k}) && (37)\\
&= 2\pi\sigma_1^2 \sum_k \mu^{\{1,\sigma_1\}}(x_k, y_k) f(x_{l-k}, y_{l-k}) && (38)
\end{aligned}$$

which is an ordinary convolution of the original image with the discrete kernel $\mu^{\{1,\sigma_1\}}(x_k, y_k)$. Because of their separability, convolutions with such kernels can be implemented efficiently as a cascade of 1-D convolutions.

The function $h(x, y) = ((D_x + iD_y)f)^2$ is non-linear in f and it will be referred to as the Infinitesimal Linear Symmetry (ILS) image. This is computed as a point-wise squaring

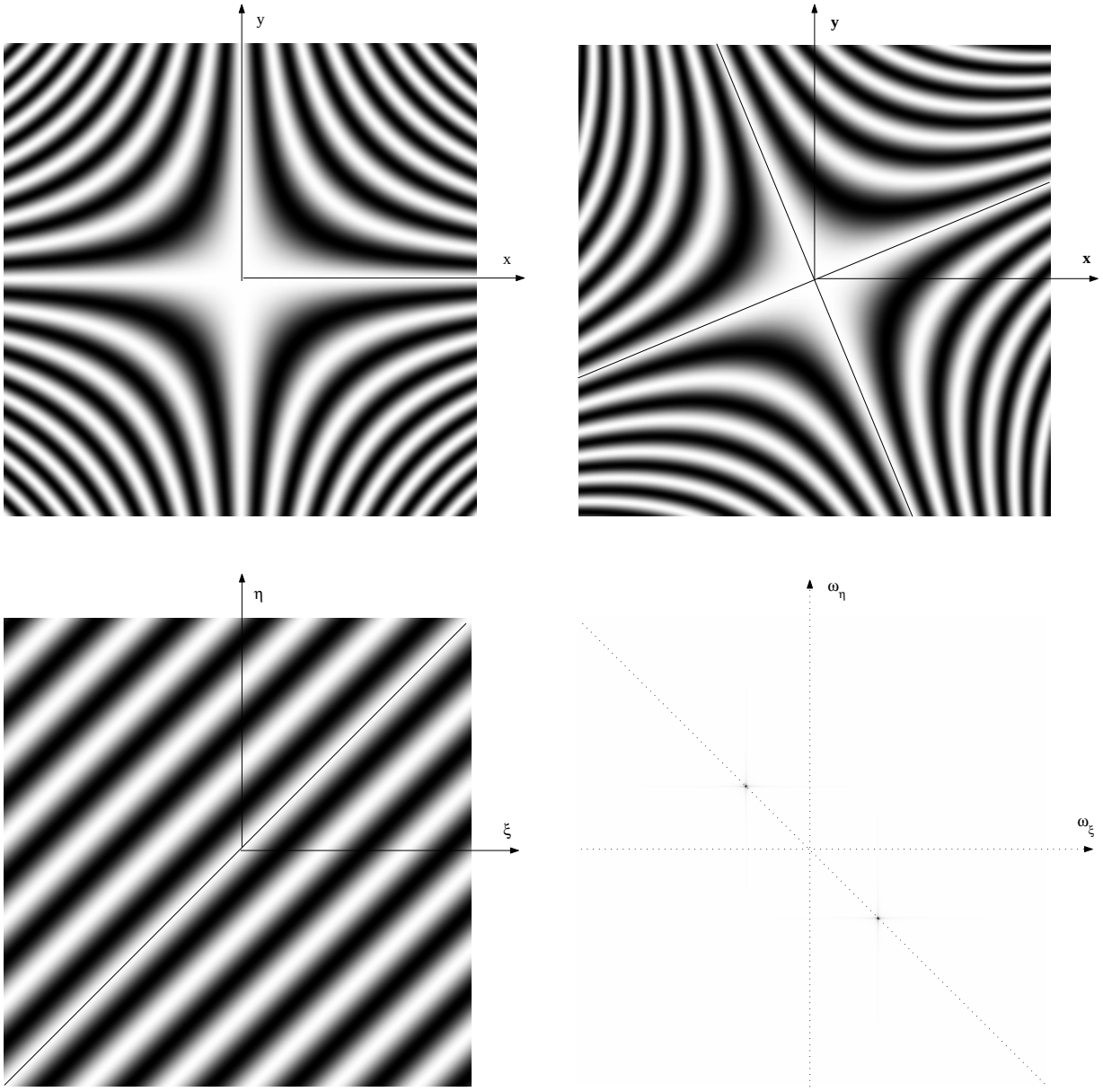

Figure 3: The patterns illustrating iso gray curves that model cross markers. They are obtained by $\cos(\frac{2\pi}{1/16}(\sin(2\theta)(x^2-y^2)-\cos(2\theta)2xy))$ where the spatial measurement unit in both x and y directions is the horizontal size of the image. The function $\cos$ is here chosen for convenience as it illustrates effectively the the non-linear coordinate transformation (27–28). On top-left $\theta = 0$, and on the top-right $\theta = \frac{\pi}{8}$ are displayed. The bottom-left image represents the mapping (27–28) applied to the image on top-right whereas the bottom-right image represents the modulus of the Fourier transform of the bottom-left image taken in ξ, η coordinates.

applied to (36) which in the discrete case is approximated by applying the pixel wise squaring on the original grid: i.e. by squaring (38):

$$h(x_l, y_l) = ((D_x + iD_y)f(x_l, y_l))^2 \quad = \quad (2\pi\sigma_1^2 \sum_k \mu^{\{1,\sigma_1\}}(x_k, y_k) f(x_{l-k}, y_{l-k}))^2 \tag{39}$$

On a sufficiently dense image grid, $h(x, y)$ too can be reconstructed from its samples $h(x_l, y_l)$,

$$h(x, y) \quad = \quad 2\pi\sigma_1^2 \sum_k h(x_k, y_k)\mu^{\{0,\sigma_1^2\}}(x - x_k, y - y_k) \tag{40}$$

In practice our target image is a neighborhood in a large image so that we must use a window function $w(x, y)$ that extracts the effective neighborhood, directly from the ILS image h, since this is already available for all points of the large image via (39). Thus w needs essentially to be zero outside of a support area that defines the local image. With this in mind, I_{20} is obtained as

$$I_{20}(x', y') \quad = \quad \int\int \frac{(x - iy)^2}{|x - iy|^2} w(x, y)h(x' - x, y' - y)dxdy \tag{41}$$

where w is a window function that defines the neighborhood around the origin. In the integrand h is shifted in such a way that the local image around (x', y'), the current point, is always centered at the origin.

Concerning the window function, there is room for flexibility as this is a design parameter. Here we choose it as

$$w(x, y) \quad = \quad \pi e(x^2 + y^2)\mu^{\{0,\sigma_2^2\}}(x, y) \tag{42}$$

The motivations behind this include:

1. It effectively suppresses the the origin as information provider for cross detection. The center of a cross is the only point which has not a unique orientation associated with it, causing a singularity in orientation determination. The constant πe normalizes w so that its maximum is 1.
2. It extracts the neighborhood rotation symmetrically.
3. It gives a discrete cross-tracking filter that allows implementations with separable 1-D convolutions. This is shown here next.
4. The maximum of the window function is attained on a ring with radius $\sqrt{2}\sigma_2$ that can be shifted with the design parameter σ_2.

By substituting (40) in (41) and utilizing (42) one obtains $I_{20}(x', y')$ as:

$$I_{20}(x', y') = 2\pi\sigma_1^2 \sum_k h(x_k, y_k) \int\int \frac{(x - iy)^2}{|x + iy|^2} w(x, y)\mu^{\{0,\sigma_1^2\}}(x' - x - x_k, y' - y - y_k)dxdy$$

$$= 2\pi\sigma_1^2 \sum_k h(x_k, y_k) \times$$

$$\int\int \frac{(x - iy)^2}{x^2 + y^2} \pi e(x^2 + y^2)\mu^{\{0,\sigma_2^2\}}(x, y)\mu^{\{0,\sigma_1^2\}}(x' - x - x_k, y' - y - y_k)dxdy$$

$$= 2\pi^2 e\sigma_1^2 \sum_k h(x_k, y_k) \int\int (x-iy)^2 \mu^{\{0,\sigma_2^2\}}(x,y)\mu^{\{0,\sigma_1^2\}}(x'-x-x_k, y'-y-y_k)dxdy$$

$$= 2\pi^2 e\sigma_1^2 \sum_k h(x_k, y_k) \int\int \sigma_2^4 (\frac{x-iy}{\sigma_2^2})^2 \mu^{\{0,\sigma_2^2\}}(x,y)\mu^{\{0,\sigma_1^2\}}(x'-x-x_k, y'-y-y_k)dxdy$$

$$= 2\pi^2 e\sigma_1^2\sigma_2^4 \sum_k h(x_k, y_k) \int\int \mu^{*\{2,\sigma_2^2\}}(x,y)\mu^{\{0,\sigma_1^2\}}(x'-x-x_k, y'-y-y_k)dxdy \quad (43)$$

$$= 2\pi^2 e\sigma_1^2\sigma_2^4 \sum_k h(x_k, y_k)(\mu^{*\{2,\sigma_2^2\}} * \mu^{\{0,\sigma_1^2\}})(x'-x_k, y'-y_k) \quad (44)$$

$$= 2\pi^2 e\sigma_1^2\sigma_2^4 \sum_k h(x_k, y_k)\mu^{*\{2,\sigma_1^2+\sigma_2^2\}}(x'-x_k, y'-y_k) \quad (45)$$

Here (43) is obtained by utilizing Theorem 1 and (45) is obtained by utilizing Theorem 3.

Equation (45) can be computed on the discrete grid of the original image by the substitution $(x', y') = (x_l, y_l)$:

$$\begin{aligned} I_{20}(x_l, y_l) &= 2\pi^2 e\sigma_1^2\sigma_2^4 \sum_k h(x_k, y_k)\mu^{*\{2,\sigma_1^2+\sigma_2^2\}}(x_l - x_k, y_l - y_k) \\ &= 2\pi^2 e\sigma_1^2\sigma_2^4 (h * \mu^{*\{2,\sigma_1^2+\sigma_2^2\}})(x_l, y_l) = (h * s)(x_l, y_l) \end{aligned} \quad (46)$$

which is an ordinary convolution of the discrete h with the discrete filter s:

$$s(x_l, y_l) = 2\pi^2 e\sigma_1^2\sigma_2^4 \mu^{*\{2,\sigma_1^2+\sigma_2^2\}}(x_l, y_l) \quad (47)$$

Since the maximum of $|\mu^{*\{2,\sigma_1^2+\sigma_2^2\}}|$ is $(\pi e(\sigma_1^2+\sigma_2^2)^2)^{-1}$ and it is attained at the radius

$$r_0 = \sqrt{x_0^2 + y_0^2} = \sqrt{2(\sigma_1^2+\sigma_2^2)}, \quad (48)$$

the maximum of $|w|$ is also attained at the same radius which effectively determines the ring in which the information is most influential as it comes to estimate the cross fitting errors and the optimal orientation. Although not essential for our application, since we have contrast invariant likelihoods on which filter height has no influence, we note for completeness that the maximum modulus of the filter (attained on the ring r_0) is

$$|s_0| = 2\pi \frac{\frac{1}{\sigma_1^2}}{(\frac{1}{\sigma_1^2} + \frac{1}{\sigma_2^2})^2} \quad (49)$$

Since we assumed that σ_1 controls the interpolation function and σ_2 controls the window function it follows that in practice we have $\sigma_1 << \sigma_2$. This in turn results in that the maximum magnitude of the filter is determined by the parameter σ_1, see (49), and the radius of the maximum is determined by σ_2, see (48).

Filtering with s can be implemented as the sum of 3 separable filters since

$$\begin{aligned} \mu^{*\{2,\sigma_1^2+\sigma_2^2\}})(x_l, y_l) &= (\frac{x-iy}{\sigma_1^2+\sigma_2^2})^2 \exp(-\frac{x_l^2}{2(\sigma_1^2+\sigma_2^2)}) \exp(-\frac{y_l^2}{2(\sigma_1^2+\sigma_2^2)}) \\ &= \frac{x^2-y^2+i2xy}{(\sigma_1^2+\sigma_2^2)^2} \exp(-\frac{x_l^2}{2(\sigma_1^2+\sigma_2^2)}) \exp(-\frac{y_l^2}{2(\sigma_1^2+\sigma_2^2)}) \end{aligned} \quad (50)$$

Here, we note that, a filtering scheme that makes use of filters similar to that of Equation (50) has recently been suggested by [21] without the symmetry properties of the Gaussian derivatives.

With an analogous reasoning one arrives at that $I_{11}(x_l, y_l)$ yields

$$I_{11}(x_l, y_l) \quad = \quad 2\pi^2 e \sigma_1^2 \sigma_2^4 (|h| * |\mu^{*\{2,\sigma_1^2+\sigma_2^2\}}|)(x_l, y_l) = (|h| * |s|)(x_l, y_l) \qquad (51)$$

which is an ordinary convolution of the discrete $|h|$ with the discrete filter $|w|$. The discrete functions h and s are defined as before i.e. via (39) and (47) respectively. Filtering with $|s|$ can be achieved with 2 separable convolutions since

$$\begin{aligned} |\mu^{*\{2,\sigma_1^2+\sigma_2^2\}})(x_l, y_l)| &= (\frac{|x-iy|}{\sigma_1^2+\sigma_2^2})^2 \exp(-\frac{x_l^2}{2(\sigma_1^2+\sigma_2^2)}) \exp(-\frac{y_l^2}{2(\sigma_1^2+\sigma_2^2)}) \\ &= \frac{x^2+y^2}{(\sigma_1^2+\sigma_2^2)^2} \exp(-\frac{x_l^2}{2(\sigma_1^2+\sigma_2^2)}) \exp(-\frac{y_l^2}{2(\sigma_1^2+\sigma_2^2)}) \end{aligned} \qquad (52)$$

Finally, the local maximum of the relative certainty, as defined by (33) is used in order to track a cross from one image frame to the next. It is worth to note that in C_r both nominator and denominator use filters and images with identical moduli so that nominator can at most produce a complex number with a modulus equal to the denominator, which is always real. This is exactly what has been predicted by the continuous theory, (33).

Together, the equations (38), (39), (46) and (51) define a filtering scheme that have been implemented by means of separable convolutions and pixel wise complex squaring in an attempt to provide a robust and fast tracker for cross patterns. The scheme employs the discretized $\mu^{*\{p,\sigma^2\}}$ and $|\mu^{*\{p,\sigma^2\}}|$ as filters which were truncated when they had reached 0.5 % of their maxima in order to obtain FIR filters. The size of the filters, controlled by σ, were varied in such a way that they yielded a 9x9 filter in the convolution devised by (38) and a 30x30 filter in the convolutions devised by (46) and (51).

The current algorithm has been tested in numerous crash test sequences. A typical result of the cross marker recognition, superimposed to the original image, is shown in Figure 4 without orientation parameter modulation. We would like to point out that, the users are currently less interested in orientation estimation than orientation invariant position tracking. A zoomed version of the same image is nevertheless shown in Figure 5 with the estimated orientations modulating the orientations of the crosses. The x and y coordinates of Point 1, are shown in Figures 6 and 7.

The quality of both position and orientation parameters in all frames of this sequence as well as other sequences were similar to the frame shown here, the first in a sequence of 293 frames. The tracking was facilitated by that, a search was made within a neighborhood of an already (automatically) found marker. In the first frame, the user defines the region(s) of interest in which markers have to be found and tracked automatically. In nearly all inspected cases the cross markers could be tracked robustly including the longest image sequences in the order of a thousands of frames. The algorithm loses the track of a marker when the contrast level of a cross is extremely poor, due to specular reflection, very poor illumination, or very strong light.

Alternatives to this approach were also considered. In particular a set of 4 Hough transforms fitting 4 individual lines have been tested. Another approach that was tested was

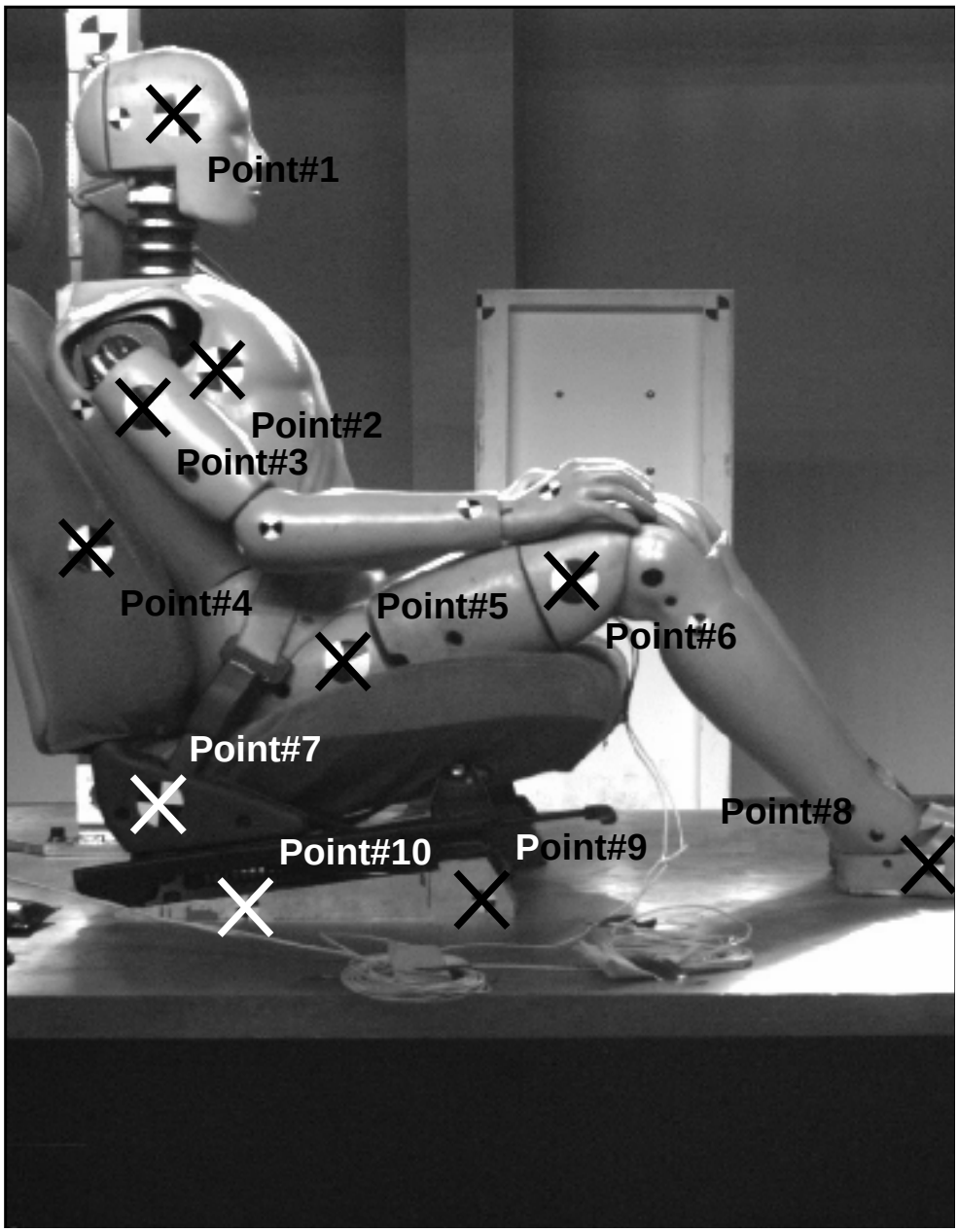

Figure 4: The figure illustrates with drawn crosses, the tracked marker positions.

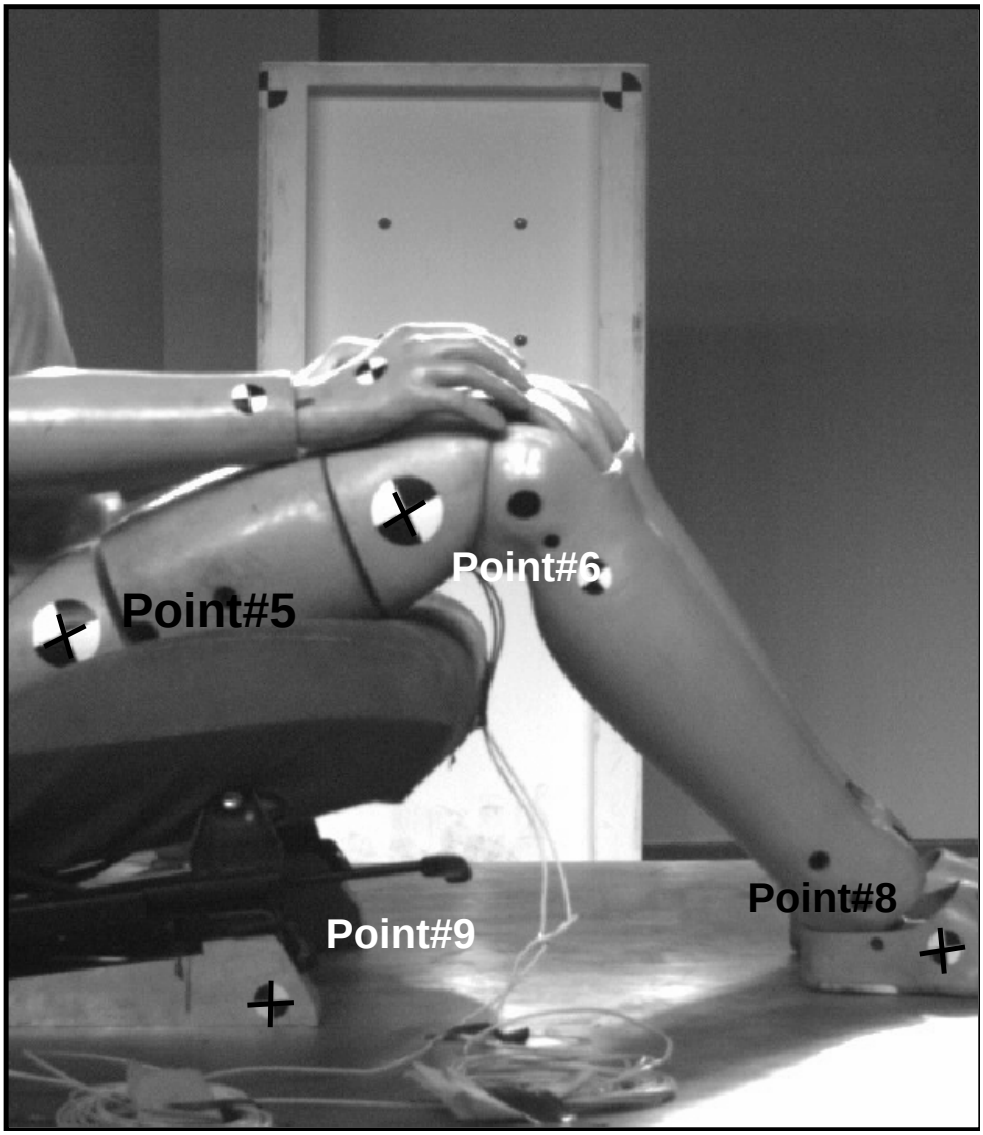

Figure 5: The figure illustrates the zoomed image superimposed with rotated crosses illustrating the positions and orientations of the tracked markers.

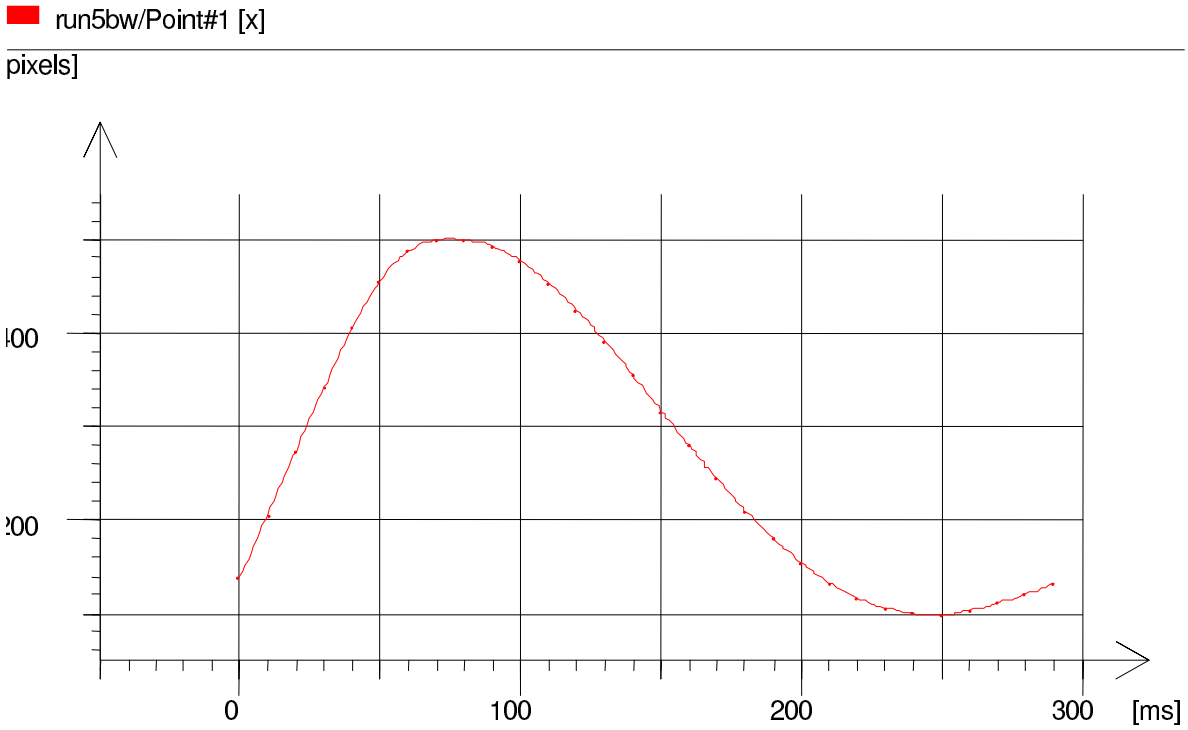

Figure 6: The figure illustrates the x coordinates of the tracked marker positions of Point 1 across the image sequence.

correlation using the last found cross marker as a template. This was deemed to be reasonable since the sequences have high temporal sampling frequencies. In both alternatives, the performance in terms of sustained tracking with high position accuracies were however inferior to the symmetry tracker described here. In the case of correlation the orientation parameter was not possible to estimate.

4 Conclusion

We have exposed a complex derivative operator that we called symmetry derivative in connection with Gaussian interpolation functions. In 3 novel theorems we have exposed some properties of this operator that are of practical importance to 2-D signal processing. We have presented an exploitation of these properties when tracking crosses in long image sequences and have illustrated them with implementation issues as well as experimental results.

Based on this, we think that the symmetry derivatives can be useful in other contexts than the one that has been presented here. One such context is detecting other symmetrical patterns than crosses, e.g. circles, radial patterns, etc. This can be done readily within the the theory presented in [3], which is an extension of the Generalized Hough transform with complex votes, and in analogy with the implementation suggested here.

As in our example application, cascades of general linear operators and pixel wise polynomial operations, can benefit from symmetry derivatives of Gaussians since these can be realized by discrete convolutions with the symmetry derivatives of Gaussians.

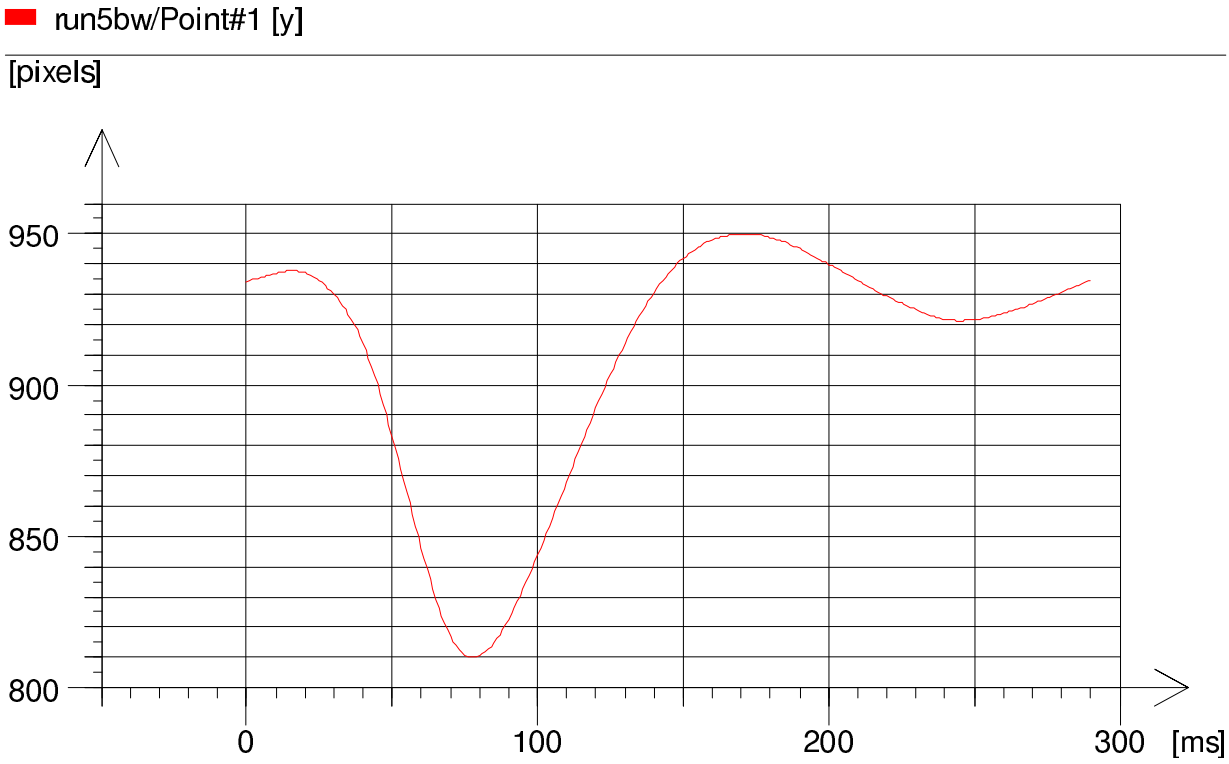

Figure 7: The figure illustrates the y coordinates of the tracked marker positions of Point 1 across the image sequence.

References

[1] J. Bigun. Recognition of local symmetries in gray value images by harmonic functions. In *Ninth International Conference on Pattern Recognition, Rome*, pages 345–347. IEEE Computer Society Press, November 14–17 1988.

[2] J. Bigun. A structure feature for some image processing applications based on spiral functions. *Computer Vision, Graphics, and Image Processing*, 51(2):166–194, August 1990.

[3] J. Bigun. Pattern recognition in images by symmetries and coordinate transformations. *Computer Vision and Image Understanding*, 68(3):290–307, 1997.

[4] J. Bigun and J. M. H. du Buf. N-folded symmetries by complex moments in Gabor space. *IEEE-PAMI*, 16(1):80–87, 1994.

[5] J. Bigun and G. H. Granlund. Optimal orientation detection of linear symmetry. In *First International Conference on Computer Vision, ICCV (London)*, pages 433–438, Washington, DC., June 8–11 1987. IEEE Computer Society Press.

[6] J. Bigun, G. H. Granlund, and J. Wiklund. Multidimensional orientation estimation with applications to texture analysis and optical flow. *IEEE-PAMI*, 13(8):775–790, August 1991.

[7] H. Burkhardt. *Transformationen zur lageinvarianten Merkmalgewinnung.* PhD thesis, Habilitationsschrift, Univesitaet Karlsruhe, Ersch. als Fortschrittbericht (Reihe 10, Nr.7) der VDI-Zeitschriften, VDI-Verlag., 1979.

[8] P. Burt. Fast filter transforms for image processing. *Computer graphics and image processing*, 16:20–51, 1981.

[9] J. F. Canny. Finding edges ond lines. Technical Report 20, Massachusetts Institute of Technology, 1983.

[10] P.E. Danielsson. Rotation invariant linear operators with directional response. In *Proceedings of 5'th international conference on pattern recognition, ICPR-80, Miami Beach, Florida, December*, pages 1171–1176. IEEE Computer Society Press, 1980.

[11] L.M.J. Florack, B.M. ter H. Romeny, J.J. Koenderink, and M.A. Viergever. General intensity transformations and second order invariants. In *7'th Scandinavian conference on image analysis, Aalborg, 13-16 august*, pages 338–345, 1991.

[12] L.M.J. Florack, B.M. ter H. Romeny, J.J. Koenderink, and M.A. Viergever. Families of tuned scale-space kernels. In ed. G. Sandini, editor, *ECCV92, Santa Margherita, Italy, May*, pages 19–23. Springer, 1992.

[13] G. H. Granlund. Fourier preprocessing for hand print character recognition. *IEEE trans. Computers*, 21:195–201, 1972.

[14] G. H. Granlund. In search of a general picture processing operator. *Computer Graphics and Image Processing*, 8(2):155–173, October 1978.

[15] G. H. Granlund H. Knutsson, M. Hedlund. Apparatus for determining the degree of consistency of a feature in a region of an image that is divided into discrete picture elements. In *US. patent, 4.747.152, Filed 1986*, 1988.

[16] O. Hansen and J. Bigun. Local symmetry modeling in multi-dimensional images. *Pattern Recognition Letters*, 13:253–262, 1992.

[17] C. Harris and M. Stephens. A combined corner and edge detector. In *Proceedings of the 4'th Alvey Vision Conference, September*, pages 147–151, 1988.

[18] L. Hong, Y. Wand, and A.K. Jain. Fingerprint image enhancement: algorithm and performance evaluation. *IEEE-PAMI Transactions on Pattern Analysis and Machine Intelligence*, 20(8):777–789, 1998.

[19] M. K. Hu. Visual pattern recognition by moment invariants. *IRE Tr. on information Theory*, pages 179–187, 1962.

[20] B. Jähne. *Digital Image Processing.* Springer-Verlag, Berlin, 4th edition, 1997.

[21] B. Johansson. *multiscale curvature detection in computer vision.* Tekn. Lic. thesis, Linkoping University, Dep. Electrical Eng., SE-581 83, 2001.

[22] M. Kass and A. Witkin. Analyzing oriented patterns. *Computer Vision, Graphics, and Image Processing*, 37:362–385, 1987.

[23] H. Knutsson. *Filtering and reconstruction in image processing.* PhD Thesis no:88, Linköping University, ISY Bildbehandling S-581 83 Linkoeping, 1982.

[24] H. Knutsson. Representing local structure using tensors. In *Proceedings 6th Scandinavian conf. on Image Analysis,*, pages 244–251, Oulu, Finland, june 1989.

[25] J. J. Koenderink and A. J. van Doorn. The structure of images. *Biological cybernetics*, 50:363–370, 1984.

[26] T. Lindeberg. *Discrete scale-space theory and the scale space primal sketch.* PhD thesis, Royal Inst. of Technology, NADA-CVAP S-100 44, Stockholm, 1991.

[27] B. D. Lucas and T. Kanade. An iterative image registration technique with an application to stereo vision. In *Proceedings of the 7´th int. joint conference on artificial intelligences, Vancouver, Canada*, pages 674–679, 1981.

[28] K. V. Mardia. *Statistics of directional data.* Academic Press, 1972.

[29] D. Marr and E. Hildreth. Theory of edge detection. *Proceedings Royal Society of London Bulletin*, 204:301–328, 1979.

[30] A. R. Rao. *A taxonomy for texture description and identification.* Springer, 1990.

[31] M. Unser, A. Aldroubi, and M. Eden. Fast b-spline transforms fo continuous image representation and intepolation. *IEEE-PAMI Transactions on Pattern Analysis and Machine Intelligence*, 13(3):277–285, march 1991.

[32] A. P. Witkin. Scale-space filtering. In *Proc. of the 8'th int. joint conf. on Artificial intelligence , Karlsruhe, Germany, August 8-12*, pages 1019–1022, 1983.